Bone 83 (2016) 65–72

Contents lists available at ScienceDirect

Bone

journal homepage: www.elsevier.com/locate/bone

Original Full Length Article

Transport of membrane-bound mineral particles in blood vessels during chicken embryonic bone development

Michael Kerschnitzki [a,*], Anat Akiva [a], Adi Ben Shoham [b], Naama Koifman [c], Eyal Shimoni [d], Katya Rechav [d], Alaa A. Arraf [e], Thomas M. Schultheiss [e], Yeshayahu Talmon [c], Elazar Zelzer [b], Stephen Weiner [a], Lia Addadi [a]

[a] Department of Structural Biology, Weizmann Institute of Science, 76100 Rehovot, Israel
[b] Department of Molecular Genetics, Weizmann Institute of Science, 76100 Rehovot, Israel
[c] Department of Chemical Engineering and the Russell Berrie Nanotechnology Institute (RBNI), Technion-Israel Institute of Technology, Haifa 32000, Israel
[d] Department of Chemical Research Support, Weizmann Institute of Science, 76100 Rehovot, Israel
[e] Department of Genetics and Developmental Biology, Rappaport Faculty of Medicine, Technion-Israel Institute of Technology, 32000, Haifa, Israel

ARTICLE INFO

Article history:
Received 29 June 2015
Revised 13 October 2015
Accepted 14 October 2015
Available online 19 October 2015

Keywords:
Biomineralization
Calcium phosphate
Avian embryo
Cryo-electron microscopy
3D FIB

ABSTRACT

During bone formation in embryos, large amounts of calcium and phosphate are taken up and transported to the site where solid mineral is first deposited. The initial mineral forms in vesicles inside osteoblasts and is deposited as a highly disordered calcium phosphate phase. The mineral is then translocated to the extracellular space where it penetrates the collagen matrix and crystallizes. To date little is known about the transport mechanisms of calcium and phosphate in the vascular system, especially when high transport rates are needed and the concentrations of these ions in the blood serum may exceed the solubility product of the mineral phase. Here we used a rapidly growing biological model, the chick embryo, to study the bone mineralization pathway taking advantage of the fact that large amounts of bone mineral constituents are transported. Cryo scanning electron microscopy together with cryo energy dispersive X-ray spectroscopy and focused-ion beam imaging in the serial surface view mode surprisingly reveal the presence of abundant vesicles containing small mineral particles in the lumen of the blood vessels. Morphologically similar vesicles are also found in the cells associated with bone formation. This observation directly implicates the vascular system in solid mineral distribution, as opposed to the transport of ions in solution. Mineral particle transport inside vesicles implies that far larger amounts of the bone mineral constituents can be transported through the vasculature, without the danger of ectopic precipitation. This introduces a new stage into the bone mineral formation pathway, with the first mineral being formed far from the bone itself.

1. Introduction

Bone formation involves the uptake and transport of calcium and phosphate to the site of mineralization [1]. The first site of mineral deposition identified ex-vivo is within vesicles inside cells responsible for bone formation (presumably osteoblasts) [2]. The mineral phase formed in the embryonic mice investigated, is a highly disordered amorphous calcium phosphate (ACP) phase, and based on a Ca/P analysis, possibly a calcium polyphosphate [2]. During exocytosis the mineral particles lose their associated membrane [2]. In experiments performed in-vitro with osteoblast cultures, mineral particles are observed inside mitochondria and in associated intracellular vesicles [3]. These specialized vesicles translocate the highly disordered mineral through the cell and are eventually released into the extracellular space [3]. An alternative pathway for mineral transport to the extracellular matrix is via vesicles which are released from bone-forming cells. These vesicles subsequently concentrate calcium and phosphate from the extracellular space and then induce the formation of a disordered Ca and P mineral inside their membrane. These vesicles are often referred to as "matrix vesicles" [4,5].

The initial ACP phase released either directly from the cells or via matrix vesicles, penetrates into the collagenous matrix [2,6,7], where it transforms to a more ordered octacalcium phosphate-like (OCP-like) phase and then into carbonated hydroxyapatite (HAP) — the mature mineral phase of the skeleton [8]. Whereas the pathways of mineral deposition inside osteoblasts and their transfer to the mineralizing bone are better understood, little is known about how the large amounts of calcium and phosphate are transported through the organism to the bone-forming cells.

In this study we investigate the transport of bone mineral constituents through blood vessels during bone formation. The vascular system is anatomically intimately associated with bone development, presumably in part because it plays a role in supplying the ions necessary for bone mineralization. Thus it is generally observed that osteogenesis is

* Corresponding author at: Weizmann Institute of Science, Department of Structural Biology, 234 Herzl Street, Rehovot, 761000, Israel.
E-mail address: kerschnitzki@gmail.com (M. Kerschnitzki).

http://dx.doi.org/10.1016/j.bone.2015.10.009
8756-3282/

coupled with angiogenesis during bone development [9,10]. Blood and other extracellular body fluids are saturated with respect to carbonated hydroxyapatite [11] and calcium phosphate nanoclusters are present at physiological pH in natural biofluids such as milk and artificial biofluids simulating blood, urine and saliva [12,13]. The vascular system therefore has the potential to transport ions and/or ion clusters necessary for bone mineralization in solution, provided they do not precipitate. Precipitation is a real danger as the solubility of bone mineral at physiological pH is very low and thus limits the quantities that can be transported in this way [11]. Thus, proteins such as fetuin, matrix Gla-protein and osteopontin are present in body fluids, where they inhibit calcium phosphate mineral formation and prevent ectopic mineralization [14–18]. However, the ways in which transport of bone mineral constituents occurs in blood vessels are still not clear, especially during embryonic bone development when high transport rates must be achieved, possibly exceeding the quantities which can be transported as ions in solution.

To address this, we study chicken long-bone development at the femoral mid-diaphysis (mid-shaft region) during embryonic stages E16–E18. During incubation, the embryo grows rapidly, increasing many hundredfold in mass [19,20]. From embryonic stage E14 to E19, chicken long-bones roughly double their length, thickness and total amount of bone mineral [21]. This requires massive transport of calcium and phosphorous, which are derived from the yolk and the egg-shell, through the circulatory system [22,23]. On the periosteal side of the femoral long-bone, a large number of active osteoblasts form thin layers of primary bone around the pre-existing vasculature. The resulting bone, thus, features a large number of trabecular structures containing the bone vasculature within the center of each trabecular channel [24,25]. This well-defined blood vessel-bone architecture together with the high rates of calcium transport present during embryonic development greatly facilitates our investigation of the transport of bone mineral constituents through blood vessels during bone formation.

The investigation of biomineralization pathways is complicated because the minerals known to be involved are highly unstable and can dissolve during sample preparation. We therefore use analytical methods where these problems are minimized by rapidly freezing fresh samples under conditions in which crystallization of water into ice is reduced. This enables the examination of intact bone tissue in a completely hydrated state by utilizing cryogenic scanning electron microscopy (cryo-SEM) equipped with an energy dispersive x-ray spectroscopy (EDS) detector system. These analytical methods are suitable for locating and characterizing highly unstable calcium phosphate involved in the bone formation pathway. To obtain 3D information of the distribution of bone mineral, we also use the focused-ion beam (FIB-SEM) in the serial surface view (SSV) mode [26]. Here we report that membrane bound calcium phosphate mineral particles are abundant in blood vessels, and that such vesicles are also observed inside and outside the cells responsible for bone formation. These mineral-bearing vesicles may therefore fulfill a crucial role in the embryonic chick bone mineralization pathway.

2. Materials and methods

2.1. Preparation of chick embryos

Fertilized chick eggs were incubated at 38 °C under 80% humidity. Embryos were staged according to Hamburger and Hamilton [27] and femurs were surgically removed from the animal between stages 42–44 (embryonic days post fertilization: E16–E18) after cervical dislocation.

2.2. Histology, H&E and immunofluorescence assay

Chicken femurs were dissected and fixed in 4% paraformaldehyde (PFA)/PBS at 4 °C overnight and decalcified in a solution containing equal parts of 0.5 M EDTA (pH 7.4) and 4% PFA in PBS for 2 days. Then samples were incubated with 0.5 M EDTA (pH 7.4) for 4 days at 4 °C. After fixation and decalcification, tissues were dehydrated to 100% ethanol and embedded in paraffin. The embedded tissues were sectioned to 7 μm thick sections and collected on Fisherbrand Superfrost Plus slides and de-paraffinized and rehydrated to water. Hematoxylin and Eosin (H&E) staining was performed following standard protocols.

For immunofluorescence of blood vessels, antigen was retrieved in 10 mM sodium citrate buffer, pH 6, using a microwave. In order to block nonspecific binding of immunoglobulin, sections were incubated with 7% goat serum. Following blockage, sections were incubated overnight at 4 °C with a rabbit polyclonal antibody to the N-terminus of chick VE-Cadherin (1:50,000). Then, sections were washed in 0.1% Tween 20 in PBS three times for 5 min and incubated with secondary fluorescent antibody Cy3 (1:100; Jackson Laboratories) for 1 h at room temperature and washed again with PBS (three times for 5 min). The sections were subsequently stained with DAPI and washed with PBS. Slides were mounted with immuno-mount aqueous-based mounting medium.

2.3. Cryo-SEM

The femoral mid-shaft region was manually dissected transversely into approximately 200 μm thick bone sections. Sections were immersed immediately in 10% dextran (Fluka), sandwiched between two metal disks (3 mm diameter, 0.1 mm cavities on both sides) and cryo-immobilized in a high-pressure freezing device (HPM10; Bal-Tec) within 10 min after the time of death of the chicken. The high pressure applied during high pressure freezing slows down the formation of ice crystals during cooling. Thus, even in relatively thick samples such as ours, which cannot be cooled down very fast, cooling ideally transforms the water inside the tissue either into a glassy disordered phase or into very small ice crystals. This not only avoids rupture of cells and other soft tissues, but also prevents molecular displacements and even chemical reactions from occurring. The frozen samples were mounted on a holder under liquid nitrogen and transferred to a freeze fracture instrument (BAF 60; Bal-Tec) by using a vacuum cryo-transfer device (VCT 100; Bal-Tec). Samples were fractured at a temperature of −120 °C in a vacuum better than $5 \times 10{-}7$ mbar. Samples were etched for 10 min at −105 °C and observed in a Zeiss Ultra 55 SEM using a secondary electron in-lens detector and a backscattered electron in-lens detector (operating at 1.5 kV at a working distance of 2.2 mm). Samples were kept in the frozen-hydrated state using a cryo-stage at a temperature of −120 °C. For energy dispersive x-ray spectroscopy (EDS) the working distance was increased to 7.5 mm and spectra were collected under an acceleration voltage of 7 kV. Measurements were performed by Bruker Quantax microanalysis system with an AXS-XFlash® detector mounted on a Zeiss Ultra-Plus HR-SEM.

2.4. Focused-ion beam in the serial surface view mode (FIB-SSV)

For FIB-SSV samples were freeze substituted and embedded in Epon as follows: high pressure frozen samples were transferred into a 1.5 ml Eppendorf with −90 °C precooled acetone containing 2% glutaraldehyde and 2% osmium (vol/vol) inside the AFS2 freeze substitution device (Leica Microsystems, Vienna, Austria) in order to dehydrate, fix and stain the samples under cryo conditions. Samples were subsequently stored for 8 h at −90 °C. Temperature was then slowly increased to −20 °C during 15 h (−5 °C/h) and was consequently increased from −20 °C to 0 °C within only 20 min (60 °C/h). Samples were transferred to 0 °C precooled absolute ethanol containing 2% uranyl acetate for 1 h and subsequently washed twice in ethanol and acetone at room temperature. Finally samples were infiltrated with EPON starting with a 10% EPON solution in acetone at 4 °C with a 10% increase every 12 h up to 90% EPON and a final incubation of 4 days in 100% EPON solution with fresh EPON replaced daily. Embedded samples were then

polymerized at 60 °C for 48 h. After polymerization, samples blocks were trimmed, and the bone surface exposed using an Ultracut Reichert microtome (Leica Microsystems, Vienna, Austria) with a diamond knife (DiATOME AG, Biel, Switzerland). Trimmed blocks were sputter-coated with gold and subsequently transferred to the Helios Nanolab 600 (FEI, The Netherlands) dual beam microscope. The sample was elevated to the eucentric height (4.1 mm) and tilted to 52° so that the electron beam and the ion beam were focused at the same point. Blood vessel contours were identified at low magnification and a 50 × 20 × 1 μm protective patch of platinum was deposited on the area of interest. A U-shaped trench was milled around the area of interest in order to expose and polish the surface for the electron beam. The imaging was performed with 2048 × 1768 pixels per frame using a mixed secondary electrons/backscattered electrons (SE/BSE) detector. An automated SSV run was initiated with a slice thickness of 20 nm covering a total thickness of 10 μm and an x–y area of 41 × 35 μm.

3. Results

To investigate calcium and phosphate transport through the circulatory system, the locations of blood vessels within the bone tissue must be identified. We used Hematoxylin and Eosin (H&E) staining on decalcified transverse sections through the embryonic femoral mid-shaft. H&E staining reveals the characteristic reticulate fabric of the developing long-bone structures, including the positions of blood vessels (Fig. 1A-B). During the investigated embryonic stages (E16–E18) the femoral cortex is very porous, with thin layers of bone (collagen stained in red) forming a trabecular meshwork. Abundant cells (stained in light violet with their nuclei in dark violet) are present at the periosteal side (PS), filling up the extra-trabecular space, together with newly formed collagen (bright red). Further inside the cortex, bone structures are usually lined by only one layer of cells. Within each trabecular channel thin cells are present. These cells have an elongated morphology reminiscent of endothelial cells. The elongated cells form a lumen, within which erythrocytes (stained in red with dark violet nucleus) are occasionally found. To prove that these elongated cells are endothelial, antibody staining for vascular endothelial cadherin (VE-Cadherin, red) was performed (Fig. 1C–D). This demonstrates that a blood vessel is located more or less in the center of each trabecular channel.

We used cryogenic scanning electron microscopy (cryo-SEM) to investigate calcium and phosphate being transported in the blood vessels present within each trabecular channel, (Fig. 2). In cryo-SEM the blood vessels inside the trabecular bone channels can generally be identified by the extremely thin endothelial cells that constitute the lumen of the vessel (Fig. 2 A-C). Also erythrocytes (Er) are occasionally identified within the blood vessel (Fig. 2 D) by their very distinct texture, namely they completely lack internal organelles, although in the case of the avian they do possess a nucleus.

Many vesicles with typical diameters between 0.5 to 2 μm are observed inside the blood vessels (Fig. 2C, D). Surprisingly, some of these vesicles contain electron-dense granules as observed using backscattered electron detection (Fig. 2F–G). The diameters of the dense granules within the vesicles, range between 50 to 150 nm. The number of electron dense particles in the 2D fracture plane of each vesicle is

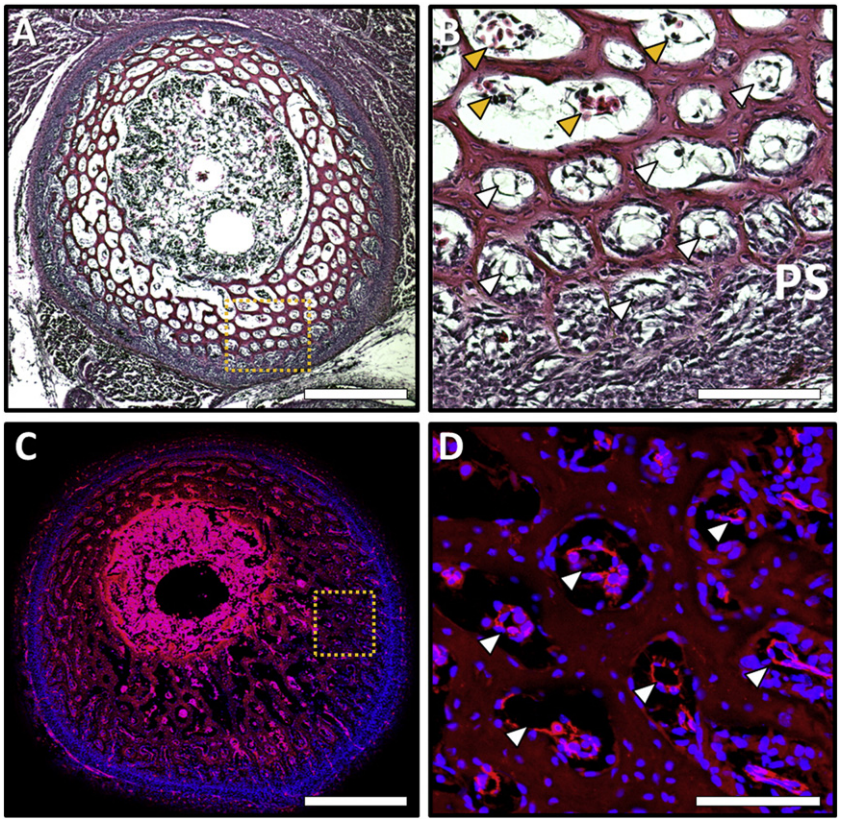

Fig. 1. Location of blood vessels within the mid-shaft region of the developing chicken femur (embryonic stage E18). (A) Hematoxylin and Eosin (H&E) staining on a decalcified section showing the growing cortex with collagen (stained in red) and cells (bright violet) with their nucleus (dark violet). (B) Magnification of area depicted by yellow box in (A) showing an abundance of cells at the periosteal side (PS) and newly formed collagen (bright red) building up the trabecular meshwork of the cortex. Note the presence of elongated thin cells reminiscent of endothelial cells confining the lumen of the blood vessel within each trabecular channel (some of these are indicated by arrowheads). Within some of the blood vessels erythrocytes (red stained cells) are observed (indicated by yellow arrowheads). (C) Immuno-staining for vascular endothelial cadherin (VE-Cadherin in red) and position of cell nuclei (DAPI, blue) in a similar transverse section. (D) Magnification of area depicted by yellow box in (C) showing that indeed a blood vessel (arrowhead) is present within each trabecular channel with the endothelial cells staining positive for VE-Cadherin (red). Scale bars: (A),(C) 400 μm; (B) 100 μm; (D) 75 μm.

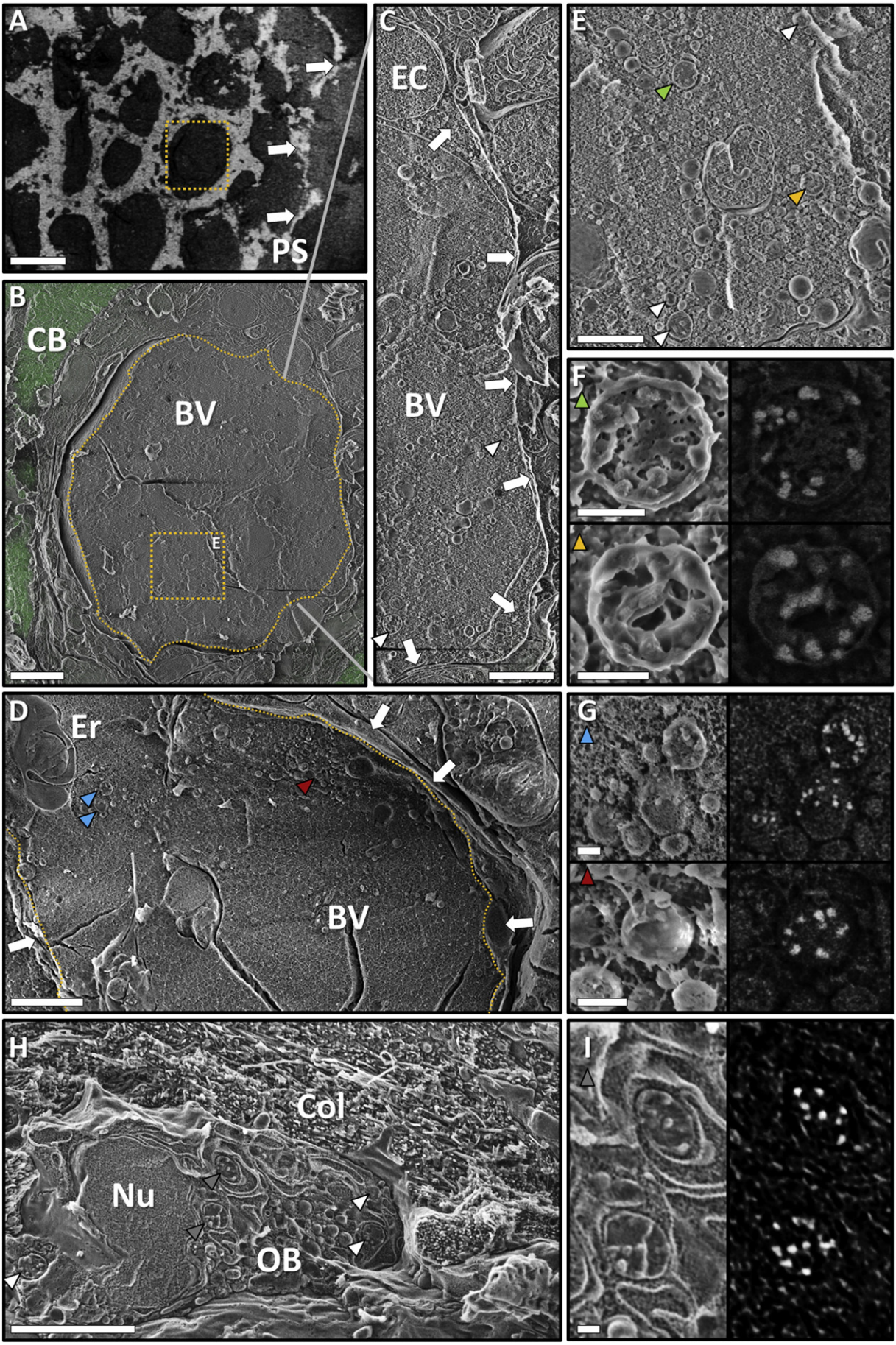
A
PS
B
CB
BV
E
C
EC
BV
E
F
D
Er
BV
G
H
Col
Nu
OB
I

around 10, and there are therefore expected to be considerably more particles in the whole vesicle. Granule-bearing vesicles and organelles are also observed in bone-forming osteoblasts in the same tissue of the chicken embryo (Fig. 2H, I), some of which have the characteristic appearance of mitochondria. The overall appearance of the granule-bearing vesicles observed in the lumen of the blood vessels and in chicken osteoblasts (excluding the mitochondria) is very similar. Similar vesicles containing granules composed of calcium and phosphorus were associated with bone-forming cells in mice embryos and zebrafish [2,6].

To determine whether membrane-bound electron-dense granules inside blood vessels are also composed of calcium and phosphate, we analyzed the ionic composition of the electron-dense granules using energy-dispersive x-ray spectroscopy (EDX) under cryogenic conditions (Figs. 3A–C). It is essential to utilize EDX under cryo-conditions as the rapid freezing procedure rules out potential positional displacements within the bone tissue. Thus it is assured that the granule-bearing vesicles observed within the lumen of the blood vessels had not artificially been moved from different tissues into the vessel. Other sample preparation procedures, such as plastic embedding following classical chemical fixation and dehydration of the sample, may cause movement of granules especially into and out of the blood vessel compartment because the blood is composed mostly of water and thus cannot be fixed as effectively as other tissues. Vesicles bearing electron-dense granules inside the blood vessels clearly show co-localized high concentrations of calcium and phosphorus, in contrast to neighboring vesicles in which these granules are absent (Fig. 3D, E). It is important to note that the measured total amount of calcium and phosphorous and thus the Ca:P ratio inside the granules cannot be reliably determined as freeze fractured samples do not possess the flat surfaces necessary for accurate quantification of the elements contained in these structures.

For a broader perspective of the 3D distribution of mineral-bearing vesicles inside blood vessels and between the blood vessel and the bone surface, we used focused ion beam serial surface view (FIB SSV) (Fig. 4). The whole FIB SSV image stack, composed of 497 images spanning a total thickness of 10 μm, is provided in the supplementary online material. High pressure frozen bone tissue was fixed with glutaraldehyde, stained with osmium and uranyl acetate and then embedded in EPON after freeze substitution of the water with ethanol and acetone. The freeze substitution sample preparation method gently replaces water with anhydrous solutions and does not dissolve transient less stable calcium phosphate precursor phases [3]. Furthermore, possible displacements of structures are minimized. Individual images from a FIB SSV stack through a blood vessel are shown at different z-positions of 0, 1.5 and 2.5 μm (Fig. 4A, B, C). These images show several mineral bearing vesicles inside the endothelial lined blood vessel. Fig. 4D–E is a z-projection that shows all the mineral-bearing vesicles inside this 2.5 μm thick stack at higher magnifications. Similar mineral-bearing vesicles are also present in the same stack at relative z-depths between 5 and 10 μm (Fig. 4F–G), but these are outside the blood vessel lumen. Such vesicles present in the extracellular space were also observed using cryo-SEM (see supplementary Fig. 1). Moreover, intracellular structures filled with mineral can be seen in Fig. 4F. These structures are reminiscent of mitochondrial networks. The cells containing these mineralized structures are located between the blood vessel and the forming bone surface. Note also that the 3D-projected mineral vesicles present inside the blood vessel and within the extracellular space are filled up with many mineral granules. (Fig. 4E, G). This is not as evident in the 2D cryo-fractures, which only show mineral granules that are exposed at the fracture surface.

4. Discussion

We show the presence of mineral-bearing vesicles inside blood vessels during embryonic chicken long-bone development. These vesicles have a distinct organization, namely they contain many individual mineral granules, each of which has a diameter of between 50 and 150 nm. In the same tissue, similar mineral-bearing vesicles are also found in bone-forming cells and occasionally outside blood vessels within the extracellular fluids. Mineral-bearing vesicles in bone-forming cells with the same or similar internal organization have been previously reported in other animals, such as during tail bone development in the zebrafish [7,28], during embryonic development of long-bones and calvaria in mice [2] and in osteoblast culture experiments [3]. The membrane-bound mineral granules in embryonic mice calvaria were found to be composed of an aggregate of smaller sub-particles [2,7]. The observations that similar granule-bearing vesicles are present in blood vessels raise the intriguing possibility that a transport mechanism exists that involves pre-formed membrane-bound mineral particles in blood vessels which are translocated towards the bone-forming cells. This may be an additional pathway to the previously proposed transport mechanism of mineral ions in solution (as opposed to mineral granules) in the blood vessel to the bone formation site [3,29,30].

There are many reports of an intimate association of vasculature with forming bones at the ultrastructural level [1,9,10,31]. The formation and stabilization of calcium phosphate nanoclusters in blood due to interaction with proteins such as phosphopeptides, fetuin and osteopontin, has also been described [12,32,33]. To our knowledge the presence of membrane bound mineral granules much larger than ion clusters in blood vessels, has not been reported. This is not surprising, because observations of such granules in the blood vessels require special preparation methods, which prevent dissolution or displacement of the very unstable mineral structures. The cryo-SEM techniques used here only recently achieved the level of resolution required for the observation and characterization of such nano-particles.

In the zebrafish caudal fin bone, calcein-stained mineral aggregates with features characteristic of an octacalcium phosphate-like (OCP) phase were observed in close proximity to blood vessels [28], but not within the blood vessels. Interestingly, some of these cells containing mineral, also show specific endothelial markers [28]. Moreover, it was observed that the calcium binding dye calcein that was injected directly into the blood stream reached and stained the tail fin bones within minutes [28]. This supports the observation that blood circulation and calcium transport are closely related.

Fig. 2. Vesicles containing electron-dense granules inside blood vessels using cryogenic scanning electron microscopy: (A) Back-scattered electron imaging (BSE) of a transverse section of the femoral cortex of the developing chicken femur (embryonic stage E18). BSE shows the distribution of electron dense material and thus indicates the distribution of bone mineral. Arrows depict newly formed, mineralizing bone structures on the periosteal side (PS) of the cortex. Yellow dotted box shows the area magnified in (B). (B) Blood vessel (BV) inside the growing cortical bone (CB, green). The yellow dotted line shows the periphery of the lumen of the BV, which is confined by endothelial cells (EC). (C) Magnification of the right side of the blood vessel showing the thin EC depicted by white arrows. (D) A different BV (lumen periphery depicted by yellow dotted line and EC by white arrows) also showing an erythrocyte (Er). The arrowheads show the locations of vesicles containing electron dense granules. (E) Magnification of an area in the lumen of the blood vessel in (B) marked by the yellow dotted box. Vesicles carrying electron-dense granules (blue arrowheads in (D) are observed inside the blood vessels at higher magnification (F and G). High magnification images of vesicles marked with a colored arrowhead in (D) and (E) are shown together with their BSE signal (right panel). The diameters of the granules range between 50 and 150 nm. (H)A cell, possibly an osteoblast juxtaposed to forming bone material, as inferred from the large amount of unmineralized collagen fibers (Col) in its vicinity. Arrowheads depict mineral-bearing vesicles inside the cell; Nu — nucleus of the cell. (I) Magnification of mineral vesicles (indicated by the gray arrowheads), together with their BSE signal. Note that the overall appearance of the mineral-bearing vesicles inside the cell is similar to mineral-bearing vesicles inside the BV. (A) BSE detector; (B)–(E), (H) in-lens detector; (F), (G), (I) in-lens left panel, BSE detector right panel. Scale bars: (A) 30 μm; (B), (D), (H) 5 μm; (C), (E) 2 μm; (F), (G), (I) 400 nm.

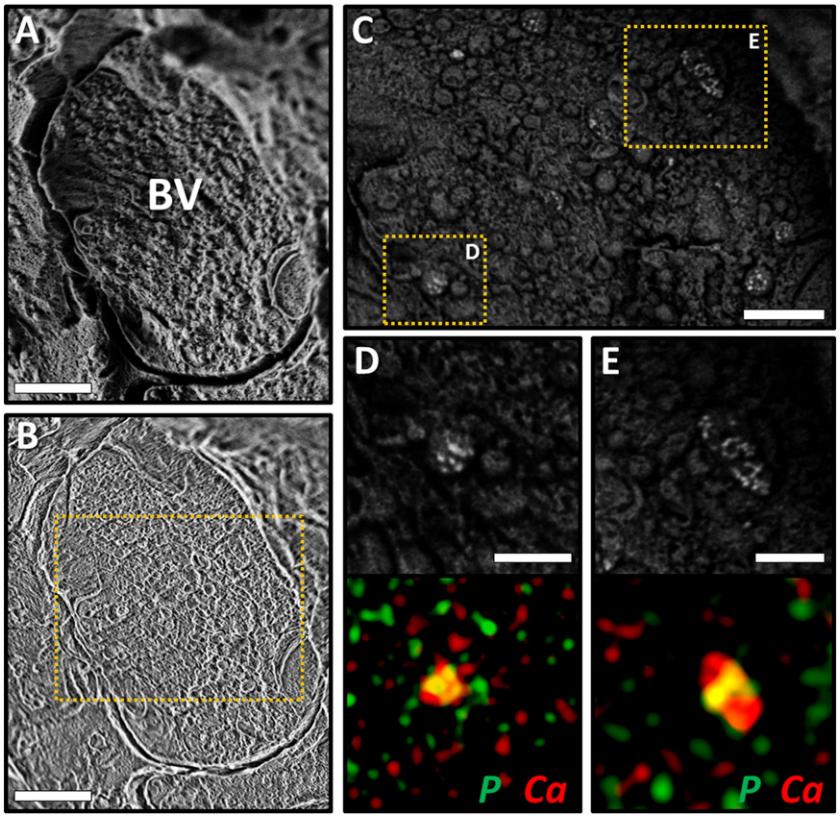

Fig. 3. Electron-dense granules contain calcium and phosphorus. Cryogenic scanning electron microscopy showing (A) the freeze-fractured surface of a blood vessel (BV) inside the growing chicken cortex measured using the secondary electron (SE) detector and (B) the in-lens detector. (C) The back-scattered electron signal of the area depicted by the yellow dotted box in (B). Vesicles bearing electron dense granules can be seen. (D) & (E) upper panels: High magnification of two of these vesicles marked with the yellow dotted boxes in (C). (D) and (E) lower panels: The distribution of calcium (red) and phosphorus (green) and both co-localized (yellow) of the same area as in the upper panels are shown. The measurements were performed by an EDS detector mounted on cryogenic high resolution SEM. Note the concentration and co-localization of calcium and phosphorus inside the vesicles with electron-dense granules, relative to the neighboring vesicles in which electron-dense granules are absent. Scale bars: (A), (B) 4 μm; (C) 2 μm; (D), (E) 1 μm.

Our finding here of membrane-bound calcium phosphate mineral within blood vessels raises the question of where such vesicles may be formed. We assume that the formation of these vesicles requires the direct involvement of cells. We can speculate about three possible locations that may be the source of these vesicles, either individually or combined:

Osteoclasts could conceivably form mineral-bearing vesicles and release them into the blood circulation. It is known that during the late stages of embryonic long-bone development in mice [34] and chicken [21,24] large numbers of active osteoclasts are present on the endosteal surface of the cortical bone. Much evidence exists that membrane bound mineral is present inside mitochondrial units in active osteoclasts [35–39] implying a storage and transport mechanism of bone mineral resorption products through the osteoclast towards the extracellular space [40]. Osteoclasts may therefore also be a source of the membrane-bound mineral particles, assuming that the mineral containing vesicles released have the same organizational structure as those observed in the blood vessels. If indeed some of the mineral bearing vesicles observed inside blood vessels are derived from osteoclasts, this process of calcium transport would be limited to bone that is undergoing high rates of resorption. Substantial bone remodeling is associated with bone formation in long-bones during embryonic growth [21,34], in medullary bone during the egg-laying cycle in avian organisms [41] and also during bone fracture healing [42].

Another possible location for the initial formation of mineral-bearing vesicles during embryonic growth may be cells located in the yolk, which is one of the major ion reservoirs for the chick embryo during incubation [43]. The yolk contains most of the P, Zn, Fe, Mn, Cu and also large amounts of calcium and these are released via the yolk sac membrane [44] during different stages of embryonic development [23]. The major source of calcium during development, however, is the egg-shell from which the embryo derives up to 80% of its total calcium [22]. Small amounts of phosphorous are also released from the eggshell [23]. Thus the cells responsible for resorbing calcium from the eggshell may also be candidates for producing the membrane-bound mineral granules. Note too, that the yolk sac membrane and also the chorioallantoic membrane covering the inner side of the eggshell are highly vascularized and facilitate the release of calcium into the circulatory system [45,46]. This pathway would, of course, be limited to animals that develop in mineralized eggs.

A third conceivable source of the granule-containing vesicles is matrix vesicles secreted from cells into the blood vessel. Matrix vesicles are 20 to 200 nm spherical bodies that arise via a budding process from the cell [28] and have been implicated in cartilage, dentine and bone mineralization [47,48]. In the extracellular space, matrix vesicles continuously concentrate calcium and phosphate from the outside environment via special ion transporters, calcium binding phospholipids and proteins, to form an amorphous calcium phosphate mineral phase [4,47]. Thus, our observations may be connected to matrix vesicles containing calcium phosphate particles probably in a disordered form. We note however that with typical diameters between 0.5 to 2 μm, the mineral-bearing vesicles we find inside the blood vessel are significantly larger than the reported size of matrix vesicles [28,48].

The utilization of mineral bearing vesicles for mineral transporters inside the serum is advantageous as, this way, the amount of calcium and phosphorous that can be transported is not limited by the solubility

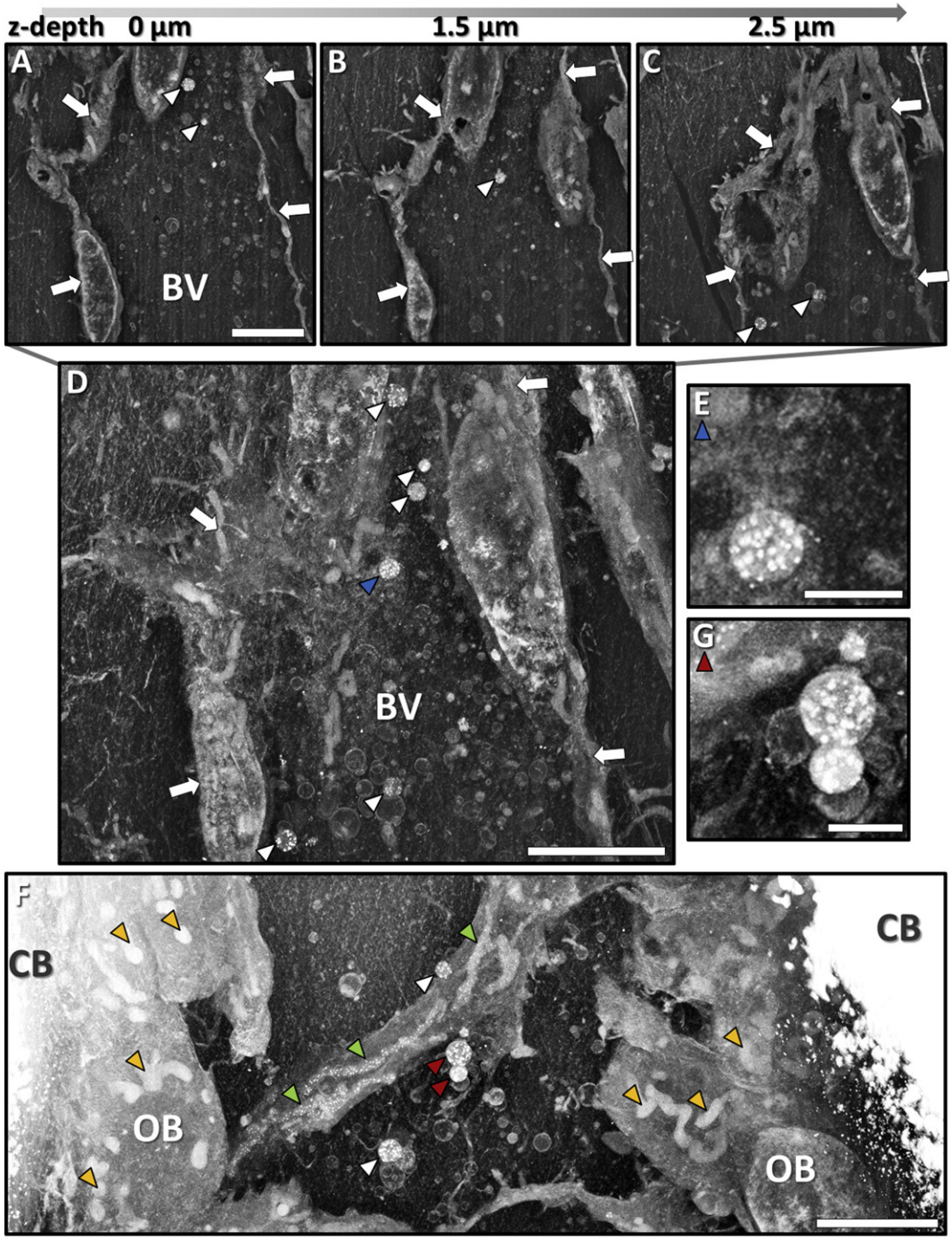

Fig. 4. 3-dimensional distribution of mineral bearing vesicles inside and outside a blood vessel. (A–C) Individual images from a focused ion beam serial surface view (FIB SSV) stack. The BV boundary is delineated by the endothelial cells (arrows) and mineral-bearing vesicles (arrowheads) can be seen inside the BV. (A), (B) and (C) are at relative z-depths of 0, 1.5 and 2.5 µm, respectively. (D) 3D-projection of the 2.5 µm of this FIB-SSV stack through the blood vessel showing all the mineral-bearing vesicles (arrowheads) and the endothelial cells (arrows). (E) Magnification of mineral-bearing vesicle indicated by blue arrowhead in (D). (F) 3D-projection of the same stack at a relative z-depth of 5–10 µm showing the BV, and the cells between the BV and the cortical bone (CB). Note the extracellular mineral-bearing vesicles (white arrowheads) which show a similar morphology to the mineral-bearing vesicles found inside blood vessels. Also note elongated intracellular organelles, reminiscent of mitochondrial networks carrying mineral particles (green arrowheads) inside cell processes connecting the cells (presumably osteoblasts (OB)) which line the mineralizing cortical bone structures. These osteoblasts possess many mitochondrial networks (yellow arrowheads), however due to insufficient contrast mineral granules are only faintly visible in these mitochondria. (G) Magnification of mineral-bearing vesicles depicted by red arrowheads in (F). Scale bars: (A)–(D), (F) 5 µm; (E), (G) 1 µm.

product of these ions in the blood serum. We also note that by isolating the mineral as solid particles in vesicles, the chance of forming ectopic calcification [49–51] of blood vessels and other soft tissues in contact with the serum is reduced. This may be another mechanism of minimizing pathology alongside other strategies of mineral nano-cluster formation by proteins present inside the serum [15,33].

5. Conclusions

We have identified mineral-bearing vesicles inside blood vessels during chicken embryonic long bone development. These vesicles are similar to mineral bearing vesicles observed inside cells involved in bone formation, as well as those found within the extracellular space

between the blood vessel-bone interface, not only in the chick, but also in embryonic mice and in the continuously growing zebrafish tail [2,3,28]. The observation of mineral bearing vesicles in the blood may thus introduce a new stage into the bone mineral formation pathway, at least in chick embryos. The existence of such mineral-bearing vesicles, especially in the blood, however, points to a possible widespread strategy for transporting large amounts of calcium through the organism with reduced risks of ectopic mineralization of soft tissues. This mechanism may be relevant not only to embryonic avian long-bone development, but also in other developmental stages and organisms.

Acknowledgments

We thank Lyad Zamir, Eldad Tzahor and Karina Yaniv (Department of Biological Regulation, Weizmann Institute of Science) for the help with chicken embryos and fruitful discussions. We thank the Irving and Cherna Moskowitz Center for Nano and Bio-Nano Imaging (Weizmann Institute of Science). The cryo-EDS work was performed in the Laboratory for Electron Microscopy of Soft Materials, supported by the Technion Russell Berrie Nanotechnology Institute (RBNI).This research was supported in part by a German Research Foundation grant, within the framework of the Deutsch-Israelische Projektkooperation. M.K. is supported by a Minerva Foundation postdoctoral fellowship. L.A. is the incumbent of the Dorothy and Patrick Gorman Professorial Chair of Biological Ultrastructure, S.W. is the incumbent of the Dr. Trude Burchardt Professorial Chair of Structural Biology.

Supplementary data to this article can be found online at http://dx.doi.org/10.1016/j.bone.2015.10.009.

References

[1] A. Posner, F. Betts, et al., Properties of nucleating systems, Metab. Bone Dis. Relat. Res. 1 (2) (1978) 179–183.
[2] J. Mahamid, A. Sharir, et al., Bone mineralization proceeds through intracellular calcium phosphate loaded vesicles: a cryo-electron microscopy study, J. Struct. Biol. 174 (3) (2011) 527–535.
[3] S. Boonrungsiman, E. Gentleman, et al., The role of intracellular calcium phosphate in osteoblast-mediated bone apatite formation, Proc. Natl. Acad. Sci. (2012) 201208916.
[4] L.N. Wu, B.R. Genge, et al., Physicochemical characterization of the nucleational core of matrix vesicles, J. Biol. Chem. 272 (7) (1997) 4404–4411.
[5] H.C. Anderson, R. Garimella, et al., The role of matrix vesicles in growth plate development and biomineralization, Front. Biosci. 10 (1) (2005) 822–837.
[6] J. Mahamid, A. Sharir, et al., Amorphous calcium phosphate is a major component of the forming fin bones of zebrafish: indications for an amorphous precursor phase, Proc. Natl. Acad. Sci. 105 (35) (2008) 12748–12753.
[7] J. Mahamid, B. Aichmayer, et al., Mapping amorphous calcium phosphate transformation into crystalline mineral from the cell to the bone in zebrafish fin rays, Proc. Natl. Acad. Sci. 107 (14) (2010) 6316–6321.
[8] N.J. Crane, V. Popescu, et al., Raman spectroscopic evidence for octacalcium phosphate and other transient mineral species deposited during intramembranous mineralization, Bone 39 (3) (2006) 434–442.
[9] B.R. Olsen, A.M. Reginato, et al., Bone development, Annu. Rev. Cell Dev. Biol. 16 (1) (2000) 191–220.
[10] A.P. Kusumbe, S.K. Ramasamy, et al., Coupling of angiogenesis and osteogenesis by a specific vessel subtype in bone, Nature 507 (7492) (2014) 323–328.
[11] F.C. McLean, M.A. Hinrichs, The formation and behavior of colloidal calcium phosphate in the blood, Am. J. Physiol.–Legacy Content 121 (3) (1938) 580–588.
[12] C. Holt, E.S. Sørensen, et al., Role of calcium phosphate nanoclusters in the control of calcification, FEBS J. 276 (8) (2009) 2308–2323.
[13] C. Holt, S. Lenton, et al., Mineralisation of soft and hard tissues and the stability of biofluids, J. Struct. Biol. 185 (3) (2014) 383–396.
[14] T. Schinke, C. Amendt, et al., The serum protein α2-HS glycoprotein/fetuin inhibits apatite formation in vitro and in mineralizing calvaria cells a possible role in mineralization and calcium homeOSTASIS, J. Biol. Chem. 271 (34) (1996) 20789–20796.
[15] G. Luo, P. Ducy, et al., Spontaneous Calcification of Arteries and Cartilage in Mice Lacking Matrix GLA Protein, 1997.
[16] J. Sodek, B. Ganss, et al., Osteopontin, Crit. Rev. Oral Biol. Med. 11 (3) (2000) 279–303.
[17] M. Ketteler, P. Bongartz, et al., Association of low fetuin-A (AHSG) concentrations in serum with cardiovascular mortality in patients on dialysis: a cross-sectional study, Lancet 361 (9360) (2003) 827–833.
[18] D. Harmey, L. Hessle, et al., Concerted regulation of inorganic pyrophosphate and osteopontin by akp2, enpp1, and ank: an integrated model of the pathogenesis of mineralization disorders, Am. J. Pathol. 164 (4) (2004) 1199–1209.
[19] C.M. Vleck, D. Vleck, Patterns of metabolism and growth in avian embryos, Am. Zool. 20 (2) (1980) 405–416.
[20] M. Pines, S. Hurwitz, The role of the growth plate in longitudinal bone growth, Poult. Sci. 70 (8) (1991) 1806–1814.
[21] R. Yair, Z. Uni, et al., Bone characteristics of late-term embryonic and hatchling broilers: bone development under extreme growth rate, Poult. Sci. 91 (10) (2012) 2614–2620.
[22] K. Simkiss, Calcium in reproductive physiology (1967).
[23] R. Yair, Z. Uni, Content and uptake of minerals in the yolk of broiler embryos during incubation and effect of nutrient enrichment, Poult. Sci. 90 (7) (2011) 1523–1531.
[24] D. Pechak, M. Kujawa, et al., Morphological and histochemical events during first bone formation in embryonic chick limbs, Bone 7 (6) (1986) 441–458.
[25] D. Pechak, M. Kujawa, et al., Morphology of bone development and bone remodeling in embryonic chick limbs, Bone 7 (6) (1986) 459–472.
[26] J.A. Heymann, M. Hayles, et al., Site-specific 3D imaging of cells and tissues with a dual beam microscope, J. Struct. Biol. 155 (1) (2006) 63–73.
[27] V. Hamburger, H.L. Hamilton, A series of normal stages in the development of the chick embryo, J. Morphol. 88 (1) (1951) 49–92.
[28] A. Akiva, G. Malkinson, et al., On the pathway of mineral deposition in larval zebrafish caudal fin bone, Bone 75 (2015) 192–200.
[29] J. Mahamid, L. Addadi, et al., Crystallization Pathways in Bone, Cells Tissues Organs 194 (2–4) (2011) 92–97.
[30] S. Weiner, L. Addadi, Crystallization pathways in biomineralization, Annu. Rev. Mater. Res. 41 (2011) 21–40.
[31] E. Zelzer, B.R. Olsen, Multiple roles of vascular endothelial growth factor (VEGF) in skeletal development, growth, and repair, Curr. Top. Dev. Biol. 65 (2004) 169–187.
[32] A. Heiss, A. DuChesne, et al., Structural basis of calcification inhibition by α2-HS glycoprotein/fetuin-A formation of colloidal calciprotein particles, J. Biol. Chem. 278 (15) (2003) 13333–13341.
[33] W. Jahnen-Dechent, C. Schäfer, et al., Mineral chaperones: a role for fetuin-A and osteopontin in the inhibition and regression of pathologic calcification, J. Mol. Med. 86 (4) (2008) 379–389.
[34] A. Sharir, T. Stern, et al., Muscle force regulates bone shaping for optimal load-bearing capacity during embryogenesis, Development 138 (15) (2011) 3247–3259.
[35] F. Gonzales, M.J. Karnovsky, Electron microscopy of osteoclasts in healing fractures of rat bone, J. Biophys. Biochem. Cytol. 9 (2) (1961) 299–316.
[36] A.L. Lehninger, Mitochondria and calcium ion transport, Biochem. J. 119 (2) (1970) 129.
[37] J. Matthews, J. Martin, Intracellular transport of calcium and its relationship to homeostasis and mineralization: an electron microscope study, Am. J. Med. 50 (5) (1971) 589–597.
[38] A. Rebel, K. Malkani, et al., Osteoclast ultrastructure in Paget's disease, Calcif. Tissue Res. 20 (1) (1976) 187–199.
[39] W.J. Landis, M.C. Paine, et al., Electron microscopic observations of bone tissue prepared anhydrously in organic solvents, J. Ultrastruct. Res. 59 (1) (1977) 1–30.
[40] I. Kawahara, M. Koide, et al., The relationship between calcium accumulation in osteoclast mitochondrial granules and bone resorption, Bone 45 (5) (2009) 980–986.
[41] M. Kerschnitzki, T. Zander, et al., Rapid alterations of avian medullary bone material during the daily egg-laying cycle, Bone 69 (2014) 109–117.
[42] A. Schindeler, M.M. McDonald, et al., Bone Remodeling During Fracture Repair: The Cellular Picture, Elsevier, Seminars in cell & developmental biology, 2008.
[43] M. Richards, M. Packard, Mineral metabolism in avian embryos, Poult. Avian Biol. Rev.(United Kingdom) (1996).
[44] L. Yadgary, R. Yair, et al., The chick embryo yolk sac membrane expresses nutrient transporter and digestive enzyme genes, Poult. Sci. 90 (2) (2011) 410–416.
[45] N. Byrd, S. Becker, et al., Hedgehog is required for murine yolk sac angiogenesis, Development 129 (2) (2002) 361–372.
[46] T. Fancsi, G. Fehér, Ultrastructural studies of chicken embryo chorioallantoic membrane during incubation, Anat. Histol. Embryol. 8 (2) (1979) 151–159.
[47] C.V. Gay, H. Schraer, et al., Ultrastructure of matrix vesicles and mineral in unfixed embryonic bone, Metab. Bone Dis. Relat. Res. 1 (2) (1978) 105–108.
[48] E.E. Golub, Role of matrix vesicles in biomineralization, Biochim. Biophys. Acta Gen. Subj. 1790 (12) (2009) 1592–1598.
[49] A.M. Parfitt, Soft-tissue calcification in uremia, Arch. Intern. Med. 124 (5) (1969) 544–556.
[50] V.L. Stewart, P. Herling, et al., Calcification in soft tissues, JAMA 250 (1) (1983) 78–81.
[51] C.M. Giachelli, Vascular calcification mechanisms, J. Am. Soc. Nephrol. 15 (12) (2004) 2959–2964.